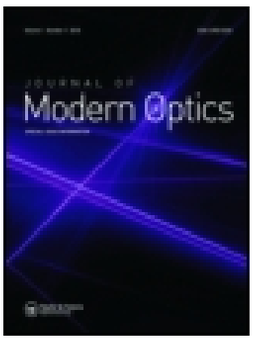

Journal of Modern Optics

ISSN: 0950-0340 (Print) 1362-3044 (Online) Journal homepage: http://www.tandfonline.com/loi/tmop20

Femtosecond X-ray-induced fragmentation of fullerenes

N. Berrah, B. Murphy, H. Xiong, L. Fang, T. Osipov, E. Kukk, M. Guehr, R. Feifel, V.S. Petrovic, K.R. Ferguson, J.D. Bozek, C. Bostedt, L.J. Frasinski, P.H. Bucksbaum & J.C. Castagna

To cite this article: N. Berrah, B. Murphy, H. Xiong, L. Fang, T. Osipov, E. Kukk, M. Guehr, R. Feifel, V.S. Petrovic, K.R. Ferguson, J.D. Bozek, C. Bostedt, L.J. Frasinski, P.H. Bucksbaum & J.C. Castagna (2015): Femtosecond X-ray-induced fragmentation of fullerenes, Journal of Modern Optics, DOI: 10.1080/09500340.2015.1064175

To link to this article: http://dx.doi.org/10.1080/09500340.2015.1064175

Journal of Modern Optics, 2015
http://dx.doi.org/10.1080/09500340.2015.1064175

Femtosecond X-ray-induced fragmentation of fullerenes

N. Berrah[a]*, B. Murphy[b], H. Xiong[a], L. Fang[c], T. Osipov[d], E. Kukk[e], M. Guehr[f], R. Feifel[g], V.S. Petrovic[f], K.R. Ferguson[d,h], J.D. Bozek[d,1], C. Bostedt[d], L.J. Frasinski[i], P.H. Bucksbaum[f] and J.C. Castagna[d]

[a]*Physics Department, University of Connecticut, Storrs, CT, USA;* [b]*Physics Department, Western Michigan University, Kalamazoo, MI, USA;* [c]*Center for High Energy Density Science, University of Texas, Austin, TX, USA;* [d]*National Accelerator Laboratory, LCLS, Menlo Park, CA, USA;* [e]*Department of Physics and Astronomy, University of Turku, Turku, Finland;* [f]*PULSE Institute, Stanford University, Stanford, CA, USA;* [g]*Physics Department, University of Gothenburg, Gothenburg, Sweden;* [h]*Department of Applied Physics, Stanford University, Stanford, CA, USA;* [i]*Department of Physics, Imperial College London, London, UK*

(*Received 10 February 2015; accepted 12 June 2015*)

A new class of femtosecond, intense, short – wavelength lasers – the free-electron laser – has opened up new opportunities to investigate the structure and dynamics in many scientific areas. These new lasers, whose performance keeps increasing, enable the understanding of physical and chemical changes at an atomic spatial scale and on the time scale of atomic motion which is essential for a broad range of scientific fields. We describe here the interaction of fullerenes in the multiphoton regime with the Linac Coherent Light Source (LCLS) X-ray free-electron laser at SLAC National Laboratory. In particular, we report on new data regarding the ionization of $Ho_3N@C_{80}$ molecules and compare the results with our prior C_{60} investigation of radiation damage induced by the LCLS pulses. We also discuss briefly the potential impact of newly available instrumentation to physical and chemical sciences when they are coupled with FELs as well as theoretical calculations and modeling.

Keywords: FEL; multiphoton; absorption; fullerene; Auger decay; radiation damage

1. Introduction

Emerging photon technologies have enabled a new class of femtosecond lasers to join the ultrafast laser family, namely the vacuum ultraviolet and X-ray free-electron lasers (FELs) operating now at several sites around the world [1–5]. They are new powerful femtosecond photonic tools, spanning a wide photon energy range, from the infra-red (IR) to the hard X-rays. One of the important attributes of these intense lasers is that they are tunable, enabling a wide class of experiments, from nonlinear science [6–29] to time-resolved dynamics in physics and chemistry [30,31]. Technological advances in building short-pulse lasers in the wavelength regime from the IR to the hard X-rays coupled with state-of-the-art instrumentation and theoretical modeling are contributing new insights to physical, chemical, and biological sciences, especially when they are paired with theoretical calculations and modeling [32–36].

Ultrafast X-rays from FELs, like synchrotron radiation, have photon energies sufficient to access core and inner-shell electrons. They are therefore different from visible optical lasers because they enable inside–out multiphoton ionization. Short-wavelength radiation can also be produced by tabletop femtosecond laser systems in the form of high harmonic generation, but the fluence in the hard X-ray regime is still weak compared to FELs [37]. X-ray absorption enables element-specificity, or in other words, one can target specific atoms within molecules or clusters and select specific shells in those atoms (by fine tuning the photon energy to specific spectral regions) [10,38]. This capability allows charting photochemical reactions and bioprocesses with atomic spatial resolution and femtosecond temporal resolution. Furthermore, the core-shell ionization and Auger decay processes, which are dominant in FEL-based work, lead to multiply charged fragments that can be compared to strong-field optical and infrared laser cases. Thus, comparisons between FEL-based and intense IR laser findings enable synergy and engagement of scientists from different communities, invigorating progress in science.

The FEL-based research in gas phase systems impacts applications ranging from single-pulse imaging of biomolecules to high-energy density materials as demonstrated by several works [11,14,15,27,29,32,33]. Coherent diffractive imaging at the atomic level requires very short and intense X-ray pulses delivered effectively by FELs to record the diffraction pattern from biological molecules before they explode due to massive Coulomb explosion [32,33,39–41]. This bioimaging has been demonstrated with resolution of tens of nanometers [42],

*Corresponding author. Email: nora.berrah@uconn.edu
[1]Curent address: SOLEIL synchrotron radiation facility, L'Orme des Merisiers Saint-Aubin - BP 48 91192 Gif-sur-Yvette, France.

but atomic resolution will require the understanding of ultrafast multiphoton ionization dynamics from inner shells which can be very well studied by atomic and molecular spectroscopic methodologies [11,14,28,30,31]. The early FEL-based experiments provided insight on the nature of the interaction of light atoms such as Ne [11] and small molecules such as N_2 [26] with intense X-ray pulses. When conducting experiments with X-ray FEL, multiphoton ionization, and subsequent Auger decay contribute substantially to what is called "electronic damage" [11,26]. This damage will deteriorate the scattering images, ultimately limiting the resolution. The earlier atomic and molecular radiation damage findings motivated in part our current work to carry out FEL-based research on intermediate size molecules such as the fullerenes because they can provide detailed information on the ionization and radiation damage mechanisms [14,16] since their size, unlike atoms [6,11–13] or small diatomic molecules [16], is closer to biosystems.

Recently, we established through work on buckminsterfullerenes (C_{60}) [14] a number of advantages for studying this sample as a benchmark case for radiation damage when compared with isolated atoms [6,11–13] small molecules [17–19,21–26] or van der Waals (vdW) clusters [27–29]. The main reason is that C_{60} consists entirely of C–C bonds and that chemically it has representative bond lengths and damage processes compared to biosystems. Furthermore, the investigation of this system is still very active because it is the basis for many novel materials such as graphene or carbon nanotubes and thus connects to many applied fields. The interaction of X-ray FELs with matter is still *terra-incognita* since these lasers are only about six years old. Furthermore, theoretical models of large molecular femtosecond dynamics under ultrafast and intense X-ray laser exposure are now available and need to be systematically tested. Our work on C_{60} [14] molecules interacting with intense X-ray pulses provided by the Linac Coherent Light Source (LCLS), revealed the influence of processes not previously reported. In particular, our joint theoretical and experimental work illustrated the successful use of classical mechanics to describe all moving particles in C_{60}, an approach that scales well to larger systems, for example, biomolecules. Understanding in detail the interaction of biomolecules with FELs is important because they are one of the poster children for the construction of FELs since they hold the promise of single molecule diffractive imaging.

From a fundamental point of view, the understanding of photo-initiated dynamics depends upon investigating the intertwined electronic and nuclear motion, which may require theoretical models beyond the Born–Oppenheimer approximation and including electron correlation. The electronic structure must be understood because it determines the potential energy surfaces along which the nuclear motion evolves. This is very difficult, however, due to the different interactions and the large number of degrees of freedom that must be considered in order to completely describe even the smallest molecule. However, molecular dynamics (MD) modeling can advance the understanding of molecular femtosecond dynamics as demonstrated in our recent work [14,16].

The need to understand intermediate size MD induced by X-ray pulses motivated the present work in endohedral fullerenes with a high Z atom because it is a model system for biomolecules such as iron-storage protein ferritin [43] and also proteins which are a large and important class of biomolecules [44]. A fundamental understanding of the electronic structure and photo-initiated nuclear dynamics in these molecules can be achieved by probing relaxation channels and reorganizational dynamics of highly excited molecules and neutral-ion charge exchange. This will enable the understanding of large organic molecules and carbon nanomaterials, important for optimizing their properties for use in molecular electronics and organic photovoltaics [45].

Our goal with the reported investigation is threefold: first, we aim to investigate the nature of the interaction and response of a large molecule, $Ho_3N@C_{80}$, with femtosecond photon pulses in order to contribute to the understanding of fundamental interactions of femtosecond X-ray pulses with complex systems such as a caged molecule; second, we attempt to shed some light onto the basic question of radiation damage and how the molecular structure changes upon intense femtosecond X-ray absorption; third, we want to compare this new work to our prior C_{60} work [14,16]. We also discuss in this manuscript the future dynamical investigations with recently emerging instrument technologies paired with ultrafast X-ray photons and modeling. Although our primary interest is of fundamental nature, our results impact matter under extreme conditions because this community interprets their data using fundamental atomic and molecular physics results [15].

2. Experimental methodology

The experiment was performed using the atomic, molecular, and optical physics instrument described in other works [11,26,46]. In particular, we used a velocity map imaging spectrometer [47] for detecting the time-of-flight (TOF) of the ions produced in the interaction of the molecules with the LCLS pulses for this experiment. The $Ho_3N@C_{80}$ molecules were collimated and introduced into the vacuum through a heated oven source. The photon energy and pulse durations are given in the results section. The pulse energy quoted is a nominal value measured upstream from the beam line optics. This value is reduced by 65–85% in the interaction

region due to photon beam transport losses [11,23,26]. The photon beam was focused by Kirkpatrick–Baez (KB) mirrors to an approximately 5 μm × 5 μm spot in the interaction chamber. For this experiment, the interaction region was downstream of the optimal X-ray beam focus, compared to our C_{60} work [14], by about 1 m because an instrument was inserted in the beamline upstream from the interaction region. This resulted in a decrease in the photon fluence.

To extract the kinetic energy (KE) of the fragment ions from their TOF data, the following procedure was used. First, the TOF responses of a specific fragment at fixed energies with isotropic spatial distribution were simulated using SIMION software; the resulting TOF responses were used as the base function for further fitting. Then, the recorded TOF data were fitted by varying the heights of those base functions. The heights, hence, the KE distribution were extracted by a genetic algorithm, which mimic the natural selection [48]. In the genetic algorithm, random sets of heights were used as the "result" from the first generation. The corresponding TOF for each "result" was calculated and its deviation from the recorded TOF data was evaluated. Those "results" with the smallest deviations were kept to produce the next generation. Mutation and crossover were applied in the production process. This generation process was iterated and stopped when further improvement was not achieved. The set of heights corresponding to the smallest deviation of the simulated TOF data to the recorded TOF data were chosen as the KE distribution. The ion yield for each fragment was volume integrated to the corresponding TOF peak. The error for each ion yield is estimated as one statistical standard deviation. For the ion fragments whose TOF peaks are mixed, the TOF peaks were fitted with Gaussian functions, and the ion yields were integrated for those Gaussian functions.

3. Results

3.1. Femtosecond molecular ionization dynamics

The dominant ionization mechanism with intense FEL is sequential multiphoton absorption as observed in several previous works on atoms, molecules, and clusters [6–29]. Multiple sequential inner-shell photoionization (P) and subsequent Auger decay (A) events, accompanied by secondary ionization processes, lead to highly charged ionic states of the target by the absorption of multiple photons from a single X-ray pulse. As the highly charged parent molecule begins to break up, it and its fragments absorb additional photons through several sequential photoionization–Auger (P–A) cycles, leading to highly charged fragment ions. These repeated P–A cycles do not occur in single-photon absorption with conventional synchrotron radiation sources. The experiment on $Ho_3N@C_{80}$ was carried out with 1530 eV. This photon energy was chosen to optimize ionization from the Ho 3d shell. In fact, the total Ho photoabsorption cross section at this photon energy is 1.5 Mb while the Ho 3d shell contributes 1.2 Mb [49]. The pulse duration was set to 80 fs and the pulse energy was nominal 2.2 mJ giving approximately 6.7 10^{18} photons/cm^2 [11, 26].

Figure 1 shows signal attributed to multiphoton ionization processes of $Ho_3N@C_{80}$. The three panels in Figure 1 show the detected ions measured with the TOF spectrometer. The top panel depicts peaks attributed to several multiply charged parent ions comprising singly charged $Ho_3N@C_{80}^{+}$ to quintuply charged $Ho_3N@C_{80}^{5+}$. We also observe the atomic Ho^+ ion which has the highest yield compared to all other ion fragments, originating from the fragmentation of the encapsulated Ho_3N molecule. The middle panel focuses on the doubly and triply ionized parent molecule along with doubly ionized fullerene molecules that lost C dimers such as $Ho_3N@C_{78}^{2+}$, $Ho_3N@C_{70}^{2+}$, and $Ho_3N@C_{50}^{2+}$; the loss of C dimers was also observed before with tabletop experiments [45]. The bottom panel shows the triply and quadruply charged parent molecules along with triply ionized parent

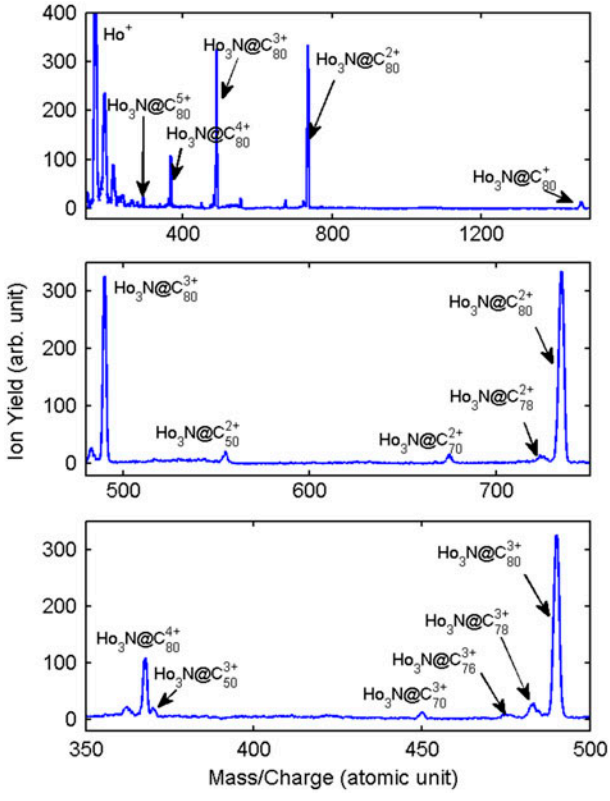

Figure 1. Ion yield M/Q spectra displayed in three panels. The top panel displays all of the ion fragments while the middle and botton fragment focus on doubly and triply charged ions (see text for details). (The color version of this figure is included in the online version of the journal.)

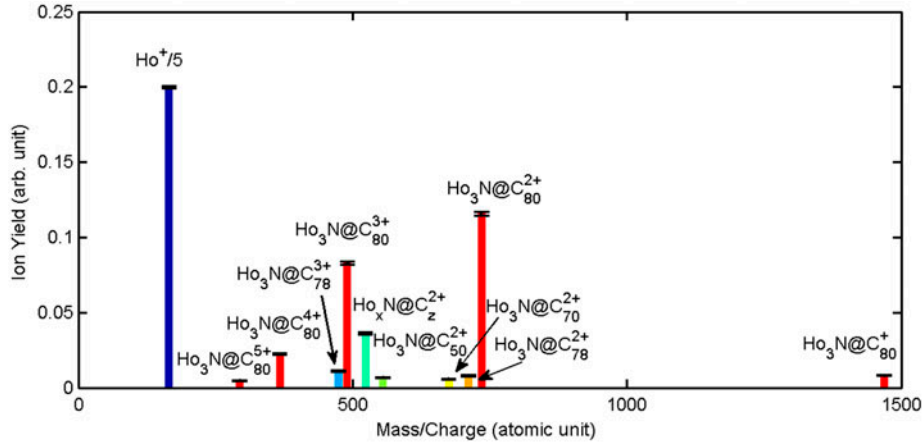

Figure 2. All measured ion yield fragments are displayed. We used different colors for the parent, atomic, and molecular fragmentions (see text for details). (The color version of this figure is included in the online version of the journal.)

molecules that lost C dimers, namely $Ho_3N@C_{78}^{3+}$, $Ho_3N@C_{76}^{3+}$, $Ho_3N@C_{70}^{3+}$, and $Ho_3N@C_{50}^{3+}$.

Figure 2 displays the entire measured fragment ions yield in one panel for ease of visualizing the ion yield of each fragment. The different colors correspond to different ion fragments labeled in the figure. As can be seen in Figure 2 the dominant ion yields are Ho^+ and the doubly and triply charged parent ions. The $Ho_xN@C_z^{2+}$ yield is in fact the sum of the fragments between $Ho_3N@C_{80}^{2+}$ and $Ho_3N@C_{50}^{2+}$ since they are not distinguishable in our experiment. We observe around the Ho^+ fragment ion a sea of singly charged molecular carbon fragment ions as shown in Figure 3.

We observe from the C_2^+ to C_{15}^+ molecular ion fragments as well as weak indication of doubly and triply charged Holmium ions, Ho^{2+} and Ho^{3+}, embedded into the singly charged carbon ion fragments. It is worth noting that the largest observed molecular carbon fragment ion is C_{24}^+, although the ion yield is small.

In order to spot other ion fragments we focus in Figure 4 on the mass-to-charge ratio between 160 and 240 and find the following Ho-based molecular fragments: HoC_2^+, $HoCN^+$, HoC_3N^+, and HoC_4^+ along with the C ion fragment. Table 1 shows the branching ratios of the observed ion fragments with respect to the dominant Ho^+ ion. The next highest ion yields after Ho^+ are C^+ and HoC_2^+.

The fragmentation dynamics of $Ho_3N@C_{80}$ also includes atomic C ion fragment shown in Figure 5, where we observe C^+, C^{2+}, and a very small amount of C^{3+}. This is unlike the case of the multiphoton ionization

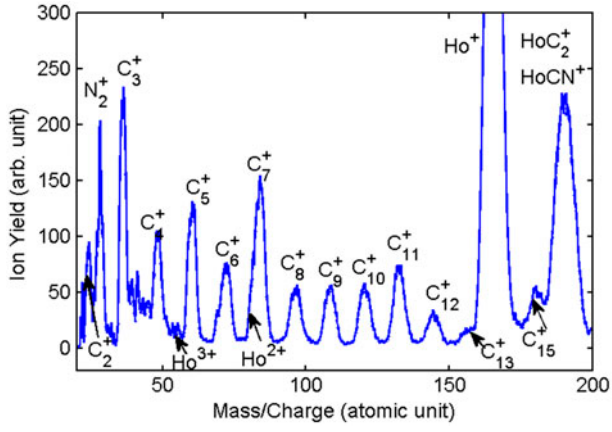

Figure 3. Ion yield displaying the molecular ion fragments and focusing on the carbon molecular ion fragments (see text for details). (The color version of this figure is included in the online version of the journal.)

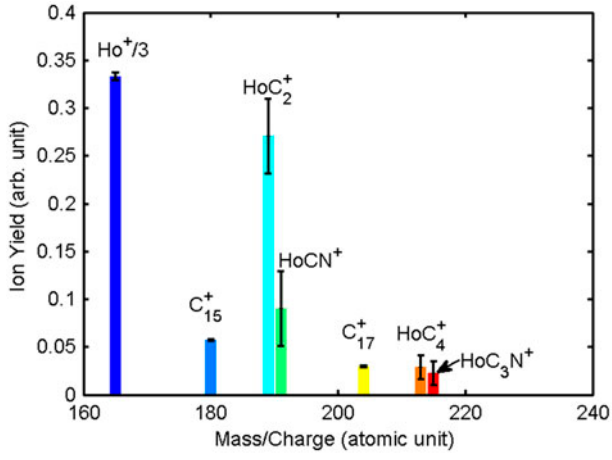

Figure 4. Ion yield fragments focusing on the atomic Ho ion and the Ho-based molecular ion fragments (see text for details). (The color version of this figure is included in the online version of the journal.)

Table 1. Normalized branch ratios (%) of selected ion fragments.

Ion	Ho^+	Ho^{2+}	$Ho_3N@C_{80}^+$	$Ho_3N@C_{80}^{2+}$	$Ho_3N@C_{80}^{3+}$	$Ho_3N@C_{80}^{4+}$	$Ho_3N@C_{80}^{5+}$
Yield (%)	100	4.8	0.83	12	8.3	2.3	0.47
Ion	C^+	C^{2+}	C^{3+}	HoC_2^+	$HoCN^+$	HoC_4^+	HoC_3N^+
Yield (%)	53	12	0.53	27	9.0	2.9	2.3

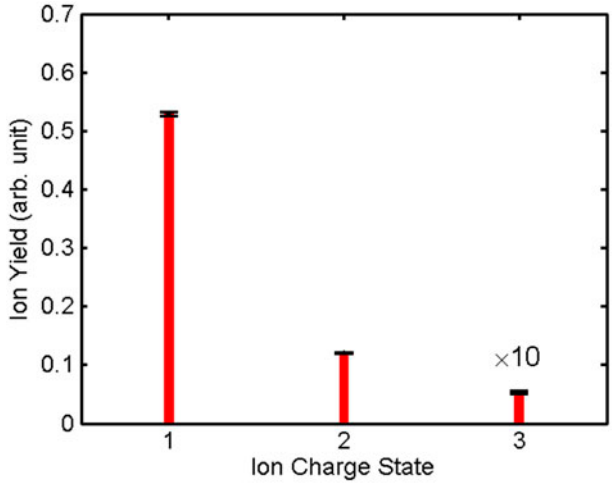

Figure 5. Carbon ion yield for the charge states of C^+ to C^{3+}. (The color version of this figure is included in the online version of the journal.)

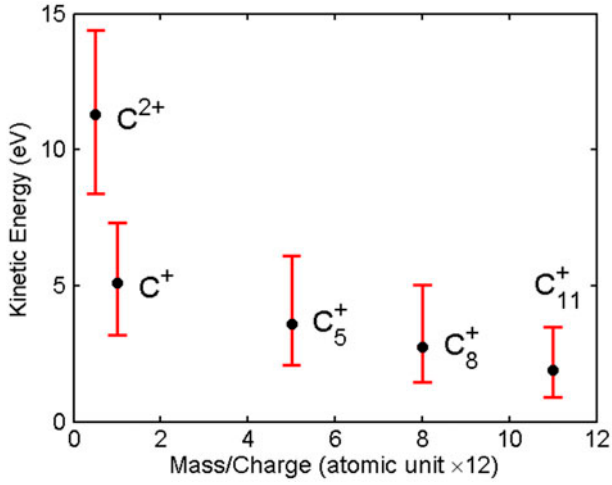

Figure 6. KE for selected atomic and molecular C fragments (see text for details). (The color version of this figure is included in the online version of the journal.)

of C_{60} at 485 eV, where for similar pulse duration (60 fs) the PAP sequence allowed the formation of up to C^{5+} [14]. We note that at the photon energy of 485 eV used in the C_{60} investigation, the photo-absorption cross section of carbon is 0.3 Mb which is much larger than 0.013 Mb at 1530 eV used in the present study. Thus, it is not surprising to only observe up to C^{3+}.

In order to understand the fragmentation dynamics and the KE sharing we analyzed the data as described above in the experimental section and plotted the kinetic energies in Figure 6, along with the error bars of the C ion fragments. It appears that C^{2+} has a greater KE than C^+ as observed in our earlier work on C_{60} [14].

We also find that the KE of singly charged carbon molecular fragments are similar to the KE of C^+. In order to understand where the deposited X-FEL pulse energy was transferred, we list in Table 2 the C and Ho fragment ion KEs along with their error bars which is large for Ho^{2+} (since it is close to the C^{7+} ion fragment as shown in Figure 3). We fit the Ho^{2+} fragment to isolate it from C^{7+}, which results in a higher uncertainty.

Since carbon ions are lighter than Ho ions, it is not surprising that their KE are larger than the Ho ions. The C KE are, however, much lower, about 10 eV for C^{2+} in the present work compared to 200 eV in the C_{60} work [14]. This is explained in Section 4.

Next, we present our data using covariance mapping [6]. This method is similar to ion–ion coincidence mapping, which connects different fragments from individual dissociation events [38,47]. However, in experiments where intense lasers are employed, many ions and electrons can be created in a single shot leading to false coincidences (combining ions from different ionized parent molecules), requiring special correction techniques. A good alternative to ion–ion coincidence is covariance mapping, where the overabundance of ions per laser pulse is much less of a problem.

To extract the correlation in such experiments, the covariance map is used to clean out false correlation in high fluence mode [6,50,51]. In practice, ions from a single shot are considered as a row vector **X(t)**. The vector is also transposed to a column vector copy, $\mathbf{Y} = \mathbf{X}^{\mathbf{T}}$. The covariance map is obtained by $\mathbf{cov<X,Y>} = \mathbf{<X \times Y>} - \mathbf{1.1} \times \mathbf{<X><Y>}$ [50], where $\mathbf{<X \times Y>}$ is the ion correlation average in single shot of all the FEL shots and $\mathbf{<X><Y>}$ is the product of averaged ion yields $\mathbf{<X>}$ and $\mathbf{<Y>}$. For practical reasons, the background suppression is enhanced by subtracting 110% of the correlation, and the diagonal line is removed for better visibility of the correlation islands.

Figure 7 shows the covariance map of the ion fragments resulting from the Coulomb explosion of $Ho_3N@C_{80}$ absorbing photons from the FEL. As we mentioned before, multiphoton absorption by Ho 3d electrons leads to a highly charged parent molecule. Similarly to C_{60}, the positive charge will be distributed

Table 2. KE of C and Ho atomic ion fragments. The upper and lower width are root-mean-squared (RMS) KE width of ions higher and lower than average KE.

	C^+	C^{2+}	Ho^+	Ho^{2+}
KE (eV) (average value)	5.1	11.3	2.0	5.3
RMS upper width (eV)	2.2	3.1	1.3	4.7
RMS lower width (eV)	1.9	2.9	0.9	2.9

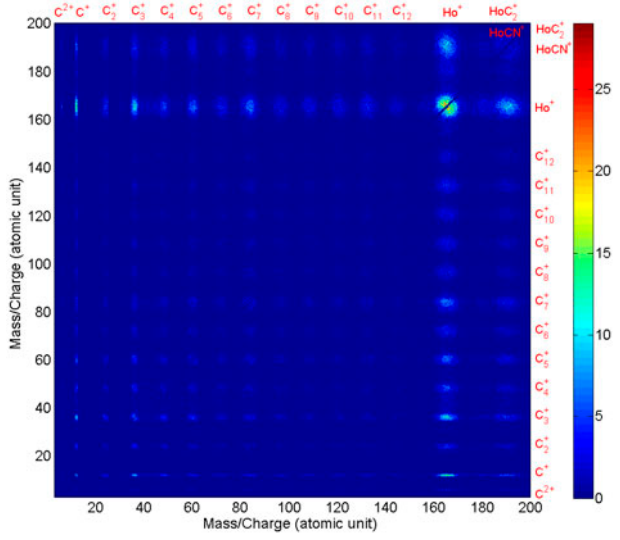

Figure 7. Mass/charge covariance map of the fragments resulting from the Coulomb explosion of Ho3N@C_{80}. (The color version of this figure is included in the online version of the journal.)

evenly [52] on the cage after the core vacancies are filled. Since the carbon cage is highly charged, many ionic carbon fragments are created in a single explosion. Thus, correlation islands of most fragment pairs are observed.

The left panel of Figure 8 presents the covariance map of small carbon fragments C_2^+ and C_3^+. A two-body Coulomb explosion would produce ions with perfectly correlated momenta, and it would be seen as a tilted line (TOF-2 vs. TOF-1) in the covariance map. If more charges and atoms are involved in the Coulomb explosion, the correlation island would be characterized by a similar slope but a broadened shape because of the momentum carried away by other fragments [47]. Total loss of correlation would result in a rectangular-shaped covariance island. Under the present experimental conditions, many bonds are broken in a single Coulomb explosion. Therefore, the correlations between the individual small carbon ionic fragments are lost, resulting in rectangular patterns.

4. Discussion

The X-ray laser parameters for the interaction of $Ho_3N@C_{80}$ are different compared to the C_{60} work carried out in the strong-fluence [14] and mid-fluence [16] regime. As mentioned above, the laser focus was weaker due to the longer path the photons had to take to reach the interaction region. In fact, we estimate that the fluence used in the $Ho_3N@C_{80}$ was only ¼ of the fluence used in C_{60} [14], resulting in only a few multiphoton ionization cycles. This estimate is supported by our data since the intensity of the peaks of the highest atomic

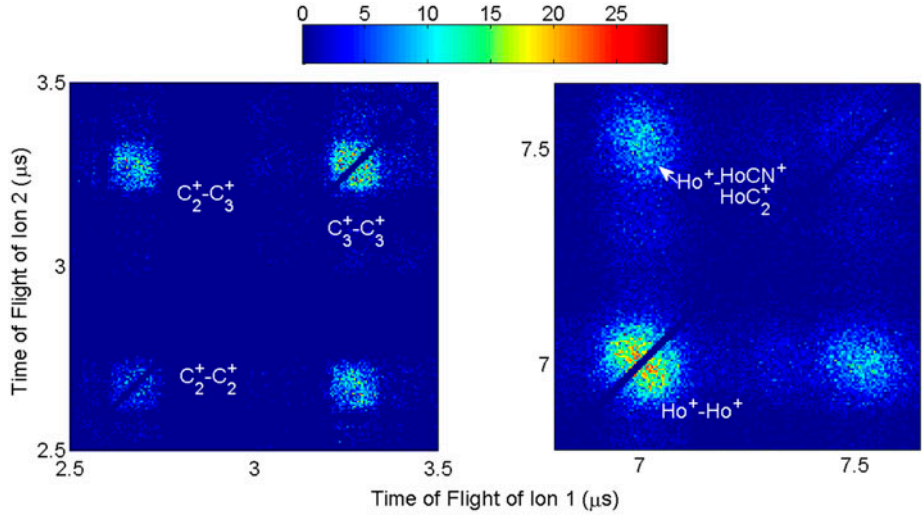

Figure 8. TOF covariance map of small molecular fragments C_2^+ and C_3^+ (left panel) and Holmium-containing internal fragments (right panel). (The color version of this figure is included in the online version of the journal.)

charge states Ho^{2+} and C^{3+}, is very little, as shown in Figure 5, compared to C^{5+} at comparable pulse duration in our previous C_{60} work [14].

In the C_{60} work, we estimated that there were 180 photons absorbed per C_{60} molecule, while only about 8 photons are absorbed by $Ho_3N@C_{80}$. This implies that in the present work we are in the low-fluence regime, where one can study the onset of fragmentation at relatively low total ion charge. Based on the absorption cross section of Ho (1.2 Mb) and C (0.013 Mb) at 1530 eV, we further estimate that Ho atoms absorb six photons while the C cage absorbs two photons in the ionization of $Ho_3N@C_{80}$. The multiphoton absorption and Auger decay cascade in Ho lead then to multiply charged parent ions. Since there is no evidence of highly charged atomic Ho fragments, this suggests that each Ho atom draws at least six electrons from the carbon cage, leading to highly charged C_{80}. Based on these estimates, our interpretation of the interaction of $Ho_3N@C_{80}$ with 1530 eV photon energy and with about 6.7×10^{18} photons/cm^2 (compared to about 5×10^{19} photons/cm^2 for the C_{60} experiment [16]) is that the parent molecule charges up and reaches at least $Ho_3N@C_{80}{}^{5+}$ as observed in Figures 1 and 2. Since the Ho atoms are about 10 times heavier than the C atoms, they will not move faster than the carbon cage. It is likely that, as the carbon cage charges up, it becomes unstable and falls apart leading to molecular fragments as shown in Figures 3 and 4. This may be followed by the break off of the three Ho atoms, due to excited state repulsion.

Figure 8 shows the Ho-containing ion fragments which are predominantly singly charged. However, Ho atom inside a cage, such as $Ho_3N@C_{80}$, has an oxidation number of +3 [53]. From a simplified ionic point of view, each Ho in $Ho_3N@C_{80}$ transfers two electrons to the C_{80} cage and one electron to N, completely filling the C_{80} HOMO cage and N valence shell. Thus, although the initial photoabsorption favors even more positive charge creation at the Ho sites, during the charge redistribution and early dissociation stages, negative charges flow into the Ho sites. Since the fragmentation of the cage occurs mostly as light fragments, and the heavier interior fragments have low charges, one can make a simple assumption: the explosion of the cage is a fast process that has little effect on the motion of the internal fragments from the viewpoint of the long-range Coulomb repulsion between fragments. In order to reliably model the fragmentation dynamics, charge transfer dynamics must be modeled first. With the absence of such modeling, only a crude interpretation can be made.

The final average KE of Ho^+ is 2.0 eV. This can be compared, as a rough estimate, to the energy released from the explosion of a triangular planar configuration of three Ho^+ ions surrounding a central N atom [54]. If we consider the Ho–N distance to be 2.1Å, based on prior work [55] and if we consider N as a neutral atom, the KE released per fragment will be 4.0 eV. However, as mentioned above, for accurate results charge migration dynamics must the known. Note that the KE distribution of Ho^+, as seen in the right panel of Figure 8, is broad. Similar to a polyatomic molecule, the correlation of Ho^+–Ho^+ ion pair is observed to be broad and clearly tilted, as shown in the right panel of Figure 8. Interestingly, similar correlation is not observed in Ho^+–(HoC_2^+, $HoCN^+$).

We assume that additional fragmentation mechanisms occur either sequentially or simultaneously because we observe in Figures 1 and 2 the parent molecule multiply ionized, having lost C atoms since we observe $Ho_3N@C_m{}^{n+}$; $n = 2$, 3 and $m = 78$, 76, 70, and 50. These weak fragments most probably lost C dimers, similar to what has been observed in previous intense IR work [45]. We also observe weak mixed molecular fragment indicating that the Ho atom formed carbon and nitrogen bonds since we observe $HoCN^+$, HoC_2^+, HoC_4^+, and HoC_3N^+ albeit in small quantities as can be seen in Figure 4. Table 1 lists the branching rations between Ho ion and some carbon and molecular fragments.

4.1. *Future research opportunities with emerging instrument technologies and improved FELs*

Femtosecond optical laser pulses have led to the development of transition state spectroscopy and femtosecond chemistry [56], and have been applied in pump-probe experiments to map out time-dependent nuclear motion in molecules [57]. Similar schemes using optical lasers and X-rays are being used with accelerator-based FELs [30,31,58], which are complementary to tabletop optical lasers offering the opportunity to interrogate MD in a site-specific manner. Furthermore, X-ray FEL-based research has already started to pursue femtosecond time-resolved experiments on bond-breaking in real time using X-ray pump X-ray probe experiments [58–60]. One scheme is to use the soft X-ray split-and-delay instrument at the AMO Hutch [61]. We plan to use this methodology to carry out time-resolved measurements on fullerenes with strong-fluence. We will use 10 fs pulse duration to conduct a virtually "jitter-free" experiment, tracking the ionization and fragmentation evolution of fullerenes. We will ionize the C cage with the first pulse and we will probe the dissociating molecules with the delayed second X-ray pulse. Our work in C_{60} predicted [14,16] that the ionization dynamics occur within the first few fs and remains into the ps regime. Such time-resolved information will be valuable in understanding the temporal development of radiation damage of medium size molecules such as C_{60}.

The past five years have been exciting with X-FEL-based experiments and the future holds many promises with the new FELs under construction around the world. Future FEL facilities are taking advantage of advances in focusing capabilities [62] and peak brightness to promise an even more robust regime of multiple photons absorbed per atom. In addition, these new facilities will provide high repetition rate, which will allow coincidence experiments [63]. Furthermore, the pulse duration is planned to be even shorter than a few femtoseconds [64], and the bandwidth will be more narrow thanks to laser or self-seeding schemes [65] allowing routine pump-probe experiments to investigate electronic and nuclear dynamics. One can also foresee that time-resolved studies with sub-fs resolution: relying on attosecond X-ray pulses at intense FELs sources will be possible using X-ray split and delay devices [55,66,67] enabling scientists to measure in real time the electron dynamics and extract the timing of many fundamental ionization processes. Coupling experimental investigations with theoretical calculations and modeling will permit the understanding of MD with atomic resolution and attosecond time structure. This achievement will be revolutionary, enabling unanticipated discoveries.

5. Conclusion

We reported in this work on the interaction of $Ho_3N@C_{80}$ at low-fluence and long pulse duration (80 fs) using the LCLS X-ray free-electron laser at SLAC National Laboratory. Under the present experimental conditions, a few multiphoton ionization cycles led to the Ho^{2+}, C^{3+} charge states, and carbon ion chains indicative of low-fluence ionization. This multiphoton ionization regime is quite different from the near complete atomization occurring at high-fluence short-pulse conditions; here one observes a more intricate dynamics with bonds breaking (Ho–N, C–C) and new bond forming (Ho–C_2, HoCN, HoC_4, and HoC_3N).

This experiment complements prior FEL experiments done at medium and high-fluence in C_{60}. Although in this case, as for C_{60}, the radiation damage at single-particle level is eventually as destructive, the full dynamics are more subtle and will likely prove to be more challenging to theoretical modeling, requiring the full inclusion of molecular potential and bonding.

Finally, inspired by our present and past results, our future plans are to investigate time-resolved ionization mechanisms of $Ho_3N@C_{80}$ at high-fluence as in the case of C_{60} [14] and compare the results to MD models, which are not yet available. We hope that our work will further stimulate and guide the development of MD simulations suitable for even larger molecules exposed to intense X-FEL pulses.

Acknowledgements

We would like to thank L. Lomb and I. Schlichting for useful insights as well as A-M Carroll for assistance with this manuscript.

Disclosure statement

No potential conflict of interest was reported by the authors.

Funding

This work was supported by the Department of Energy office of Science, Basic Energy Sciences, Division of Chemical Sciences, Geosciences, and Biosciences under [grant number DE-SC0012376]. VP and PHB were supported by the National Science Foundation. RF was supported by the Swedish Research Council (VR) and the Knut and Alice Wallenberg Foundation, Sweden.

References

[1] Berrah, N.; Bucksbaum, P.H. *Sci. Am.* **2014,** *310,* 64–71.
[2] Ackermann, W.; Asova, G.; Ayvazyan, V.; Azima, A.; Baboi, N.; Bähr, J.; Balandin, V.; Beutner, B.; Brandt, A.; Bolzmann, A.; Brinkmann, R.; Brovko, O.I.; Castellano, M.; Castro, P.; Catani, L.; Chiadroni, E.; Choroba, S.; Cianchi, A.; Costello, J.T.; Cubaynes, D.; Dardis, J.; Decking, W.; Delsim-Hashemi, H.; Delserieys, A.; Di Pirro, G.; Dohlus, M.; Düsterer, S.; Eckhardt, A.; Edwards, H.T.; Faatz, B.; Feldhaus, J.; Flöttmann, K.; Frisch, J.; Fröhlich, L.; Garvey, T.; Gensch, U.; Gerth, Ch.; Görler, M.; Golubeva, N.; Grabosch, H.-J.; Grecki, M.; Grimm, O.; Hacker, K.; Hahn, U.; Han, J.H.; Honkavaara, K.; Hott, T.; Hüning, M.; Ivanisenko, Y.; Jaeschke, E.; Jalmuzna, W.; Jezynski, T.; Kammering, R.; Katalev, V.; Kavanagh, K.; Kennedy, E.T.; Khodyachykh, S.; Klose, K.; Kocharyan, V.; Körfer, M.; Kollewe, M.; Koprek, W.; Korepanov, S.; Kostin, D.; Krassilnikov, M.; Kube, G.; Kuhlmann, M.; Lewis, C.L.S.; Lilje, L.; Limberg, T.; Lipka, D.; Löh, F.; Luna, H.; Luong, M.; Martins, M.; Meyer, M.; Michelato, P.; Miltchev, V.; Möller, W.D.; Monaco, L.; Müller, W.F.O.; Napieralski, O.; Napoly, O.; Nicolosi, P.; Nölle, D.; Nuñez, T.; Oppelt, A.; Pagani, C.; Paparella, R.; Pchalek, N.; Pedregosa-Gutierrez, J.; Petersen, B.; Petrosyan, B.; Petrosyan, G.; Petrosyan, L.; Pflüger, J.; Plönjes, E.; Poletto, L.; Pozniak, K.; Prat, E.; Proch, D.; Pucyk, P.; Radcliffe, P.; Redlin, H.; Rehlich, K.; Richter, M.; Roehrs, M.; Roensch, J.; Romaniuk, R.; Ross, M.; Rossbach, J.; Rybnikov, V.; Sachwitz, M.; Saldin, E.L.; Sandner, W.; Schlarb, H.; Schmidt, B.; Schmitz, M.; Schmüser, P.; Schneider, J.R.; Schneidmiller, E.A.; Schnepp, S.; Schreiber, S.; Seidel, M.; Sertore, D.; Shabunov, A.V.; Simon, C.; Simrock, S.; Sombrowski, E.; Sorokin, A.A.; Spanknebel, P.; Spesyvtsev, R.; Staykov, L.; Steffen, B.; Stephan, F.; Stulle, F.; Thom, H.; Tiedtke, K.; Tischer, M.; Toleikis, S.; Treusch, R.; Trines, D.; Tsakov, I.; Voge, E.; Weiland, T.; Weise, H.; Wellhöfer, M.; Wendt, M.; Will, I.; Winter, A.; Wittenburg, K.; Wurth, W.; Yeates, P.; Yurkov, M.V.; Zagorodnov, I.; Zapfe, K. *Nat. Photonics* **2007,** *1*, 336–342.
[3] Emma, P.; Akre, R.; Arthur, J.; Bionta, R.; Bostedt, C.; Bozek, J.; Brachmann, A.; Bucksbaum, P.; Coffee, R.; Decker, F.J.; Ding, Y.; Dowell, D.; Edstrom, S.; Fisher, A.; Frisch, J.; Gilevich, S.; Hastings, J.; Hays, G.; Hering,

Ph.; Huang, Z.; Iverson, R.; Loos, H.; Messerschmidt, M.; Miahnahri, A.; Moeller, S.; Nuhn, H.-D.; Pile, G.; Ratner, D.; Rzepiela, J.; Schultz, D.; Smith, T.; Stefan, P.; Tompkins, H.; Turner, J.; Welch, J.; White, W.; Wu, J.; Yocky, G.; Galayda, J. *Nat. Photonics* **2010,** *4*, 641–647.

[4] Allaria, E.; Appio, R.; Badano, L.; Barletta, W.A.; Bassanese, S.; Biedron, S.G.; Borga, A.; Busetto, E.; Castronovo, D.; Cinquegrana, P.; Cleva, S.; Cocco, D.; Cornacchia, M.; Craievich, P.; Cudin, I.; D'Auria, G.; Dal Forno, M.; Danailov, M.B.; De Monte, R.; De Ninno, G.; Delgiusto, P.; Demidovich, A.; Di Mitri, S.; Diviacco, B.; Fabris, A.; Fabris, R.; Fawley, W.; Ferianis, M.; Ferrari, E.; Ferry, S.; Froehlich, L.; Furlan, P.; Gaio, G.; Gelmetti, F.; Giannessi, L.; Giannini, M.; Gobessi, R.; Ivanov, R.; Karantzoulis, E.; Lonza, M.; Lutman, A.; Mahieu, B.; Milloch, M.; Milton, S.V.; Musardo, M.; Nikolov, I.; Noe, S.; Parmigiani, F.; Penco, G.; Petronio, M.; Pivetta, L.; Predonzani, M.; Rossi, F.; Rumiz, L.; Salom, A.; Scafuri, C.; Serpico, C.; Sigalotti, P.; Spampinati, S.; Spezzani, C.; Svandrlik, M.; Svetina, C.; Tazzari, S.; Trovo, M.; Umer, R.; Vascotto, A.; Veronese, M.; Visintini, R.; Zaccaria, M.; Zangrando, D.; Zangrando, M. *Nat. Photonics* **2012,** *6*, 699–704.

[5] Ishikawa, T.; Aoyagi, H.; Asaka, T.; Asano, Y.; Azumi, N.; Bizen, T.; Ego, H.; Fukami, K.; Fukui, T.; Furukawa, Y.; Goto, S.; Hanaki, H.; Hara, T.; Hasegawa, T.; Hatsui, T.; Higashiya, A.; Hirono, T.; Hosoda, N.; Ishii, M.; Inagaki, T.; Inubushi, Y.; Itoga, T.; Joti, Y.; Kago, M.; Kameshima, T.; Kimura, H.; Kirihara, Y.; Kiyomichi, A.; Kobayashi, T.; Kondo, C.; Kudo, T.; Maesaka, H.; Maréchal, X.M.; Masuda, T.; Matsubara, S.; Matsumoto, T.; Matsushita, T.; Matsui, S.; Nagasono, M.; Nariyama, N.; Ohashi, H.; Ohata, T.; Ohshima, T.; Ono, S.; Otake, Y.; Saji, C.; Sakurai, T.; Sato, T.; Sawada, K.; Seike, T.; Shirasawa, K.; Sugimoto, T.; Suzuki, S.; Takahashi, S.; Takebe, H.; Takeshita, K.; Tamasaku, K.; Tanaka, H.; Tanaka, R.; Tanaka, T.; Togashi, T.; Togawa, K.; Tokuhisa, A.; Tomizawa, H.; Tono, K.; Wu, S.; Yabashi, M.; Yamaga, M.; Yamashita, A.; Yanagida, K.; Zhang, C.; Shintake, T.; Kitamura, H.; Kumagai, N. *Nat. Photonics* **2012,** *6*, 540–544.

[6] Frasinski, L.J.; Zhaunerchyk, V.; Mucke, M.; Squipp, R.J.; Siano, M.; Eland, J.H.D.; Linusson, P.; Meulen, P.V.D.; Salén, P.; Thomas, R.D.; Larsson, M.; Foucar, L.; Ullrich, J.; Motomura, K.; Mondal, S.; Ueda, K.; Osipov, T.; Fang, L.; Murphy, B.F.; Berrah, N.; Bostedt, C.; Bozek, J.D.; Schorb, S.; Messerschmidt, M.; Glownia, J.M.; Cryan, J.P.; Coffee, R.N.; Takahashi, O.; Wada, S.; Piancastelli, M.N.; Richter, R.; Prince, K.C.; Feifel, R. *Phys. Rev. Lett.* **2013,** *111*, 073002.

[7] Bucksbaum, P.H.; Coffee, R.; Berrah, N. *Advances in Atomic, Molecular, and Optical Physics*; Elsevier: San Diego, CA, 2011**;** Vol. 60, Chapter 5, pp 240–289.

[8] Kanter, E.P.; Krassig, B.; Li, Y.; March, A.M.; Rohringer, N.; Santra, R.; Southworth, S.H.; DiMauro, L.F.; Doumy, G.; Roedig, C.A.; Berrah, N.; Fang, L.; Hoener, M.; Bucksbaum, P.H.; Ghimire, S.; Reis, D.A.; Bozek, J.D.; Bostedt, C.; Messerschmidt, M.; Young, L. *Phys. Rev. Lett.* **2011,** *107*, 233001.

[9] Doumy, G.; Roedig, C.; Son, S.-K.; Blaga, C.I.; DiChiara, A.D.; Santra, R.; Berrah, N.; Bostedt, C.; Bozek, J.D.; Bucksbaum, P.H.; Cryan, J.P.; Fang, L.; Ghimire, S.; Glownia, J.M.; Hoener, M.; Kanter, E.P.; Krässig, B.; Kuebel, M.; Messerschmidt, M.; Paulus, G.G.; Reis, D.A.; Rohringer, N.; Young, L.; Agostini, P.; DiMauro, L.F. *Phys. Rev. Lett.* **2011,** *106*, 083002.

[10] Berrah, N.; Bozek, J.; Costello, J.T.; Düsterer, S.; Fang, L.; Feldhaus, J.; Fukuzawa, H.; Hoener, M.; Jiang, Y.H.; Johnsson, P.; Kennedy, E.T.; Meyer, M.; Moshammer, R.; Radcliffe, P.; Richter, M.; Rouzée, A.; Rudenko, A.; Sorokin, A.A.; Tiedtke, K.; Ueda, K.; Ullrich, J.; Vrakking, M.J.J. *J. Mod. Opt.* **2010,** *57*, 1015–1040.

[11] Young, L.; Kanter, E.P.; Krässig, B.; Li, Y.; March, A.M.; Pratt, S.T.; Santra, R.; Southworth, S.H.; Rohringer, N.; DiMauro, L.F.; Doumy, G.; Roedig, C.A.; Berrah, N.; Fang, L.; Hoener, M.; Bucksbaum, P.H.; Cryan, J.P.; Ghimire, S.; Glownia, J.M.; Reis, D.A.; Bozek, J.D.; Bostedt, C.; Messerschmidt, M. *Nature* **2010,** *466*, 56–61.

[12] Rudek, B.; Son, S.K.; Foucar, L.; Epp, S.W.; Erk, B.; Hartmann, R.; Adolph, M.; Andritschke, R.; Aquila, A.; Berrah, N.; Bostedt, C.; Bozek, J.; Coppola, N.; Filsinger, F.; Gorke, H.; Gorkhover, T.; Graafsma, H.; Gumprecht, L.; Hartmann, A.; Hauser, G.; Herrmann, S.; Hirsemann, H.; Holl, P.; Hömke, A.; Journel, L.; Kaiser, C.; Kimmel, N.; Krasniqi, F.; Kühnel, K.-U.; Matysek, M.; Messerschmidt, M.; Miesner, D.; Möller, T.; Moshammer, R.; Nagaya, K.; Nilsson, B.; Potdevin, G.; Pietschner, D.; Reich, C.; Rupp, D.; Schaller, G.; Schlichting, I.; Schmidt, C.; Schopper, F.; Schorb, S.; Schröter, C.-D.; Schulz, J.; Simon, M.; Soltau, H.; Strüder, L.; Ueda, K.; Weidenspointner, G.; Santra, R.; Ullrich, J.; Rudenko, A.; Rolles, D. *Nat. Photonics.* **2012,** *6*, 858–865.

[13] Erk, B.; Boll, R.; Trippel, S.; Anielski, D.; Foucar, L.; Rudek, B.; Epp, S.W.; Coffee, R.; Carron, S.; Schorb, S.; Ferguson, K.R.; Swiggers, M.; Bozek, J.D.; Simon, M.; Marchenko, T.; Küpper, J.; Schlichting, I.; Ullrich, J.; Bostedt, C.; Rolles, D.; Rudenko, A. *Science* **2014,** *345*, 288–291.

[14] Murphy, B.F.; Osipov, T.; Jurek, Z.; Fang, L.; Son, S.-K.; Avaldi, L.; Bolognesi, P.; Bostedt, C.; Bozek, J.D.; Grilj, J.; Guehr, M.; Frasinski, L.J.; Glownia, J.; Ha, D.T.; Hoffmann, K.; Kukk, E.; McFarland, B.K.; Miron, C.; Sistrunk, E.; Squibb, R.J.; Ueda, K.; Santra, R.; Berrah, N. *Nat. Commun.* **2014,** *5,* 4281.

[15] Vinko, S.M.; Ciricosta, O.; Cho, B.I.; Engelhorn, K.; Chung, H.K.; Brown, C.R.D.; Burian, T.; Chalupský, J.; Falcone, R.W.; Graves, C.; Hájková, V.; Higginbotham, A.; Juha, L.; Krzywinski, J.; Lee, H.J.; Messerschmidt, M.; Murphy, C.D.; Ping, Y.; Scherz, A.; Schlotter, W.; Toleikis, S.; Turner, J.J.; Vysin, L.; Wang, T.; Wu, B.; Zastrau, U.; Zhu, D.; Lee, R.W.; Heimann, P.A.; Nagler, B.; Wark, J.S. *Nature* **2012,** *482*, 59–62.

[16] Berrah, N.; Fang, L.; Osipov, T.; Jurek, Z.; Murphy, B.F.; Santra, R. *Faraday Discuss*. **2014,** *171*, 471–485.

[17] Fang, L.; Rolles, D.; Rudenko, A.; Petrovich, V.; Bostedt, C.; Bozek, J.D.; Buckbaum, P.; Berrah, N. *J. Phys. B: At. Mol. Opt. Phys.* **2014,** *47*, 124006.

[18] Berrah, N.; Fang, L.; Osipov, T.; Murphy, B.; Bostedt, C.; Bozek, J.D. *J. Electron. Spectrosc. Relat. Phenom.* **2014,** *196*, 34–37.

[19] Fang, L.; Osipov, T.; Murphy, B.; Tarantelli, F.; Kukk, E.; Cryan, J.P.; Glownia, M.; Bucksbaum, P.H.; Coffee, R.N.; Chen, M.; Buth, C.; Berrah, N. *Phys. Rev. Lett.* **2012,** *109*, 263001.

[20] Murphy, B.F.; Fang, L.; Chen, M.H.; Bozek, J.D.; Kukk, E.; Kanter, E.P.; Messerschmidt, M.; Osipov, T.; Berrah, N. *Phys. Rev. A* **2012,** *86,* 053423.

[21] Salén, P.; Van der Meulen, P.; Schmidt, H.T.; Thomas, R.D.; Larsson, M.; Feifel, R.; Piancastelli, M.N.; Fang, L.; Murphy, B.; Osipov, T.; Berrah, N.; Kukk, E.; Ueda, K.; Bozek, J.D.; Bostedt, C.; Wada, S.; Richter, R.; Feyer, V.; Prince, K.C. *Phys. Rev. Lett.* **2012,** *108*, 153003.

[22] Osipov, T.Y.; Fang, L.; Murphy, B.F.; Hoener, M.; Berrah, N. *J. Phys: Conf. Ser.* **2012,** *388,* 012030.

[23] Berrah, N.; Fang, L.; Osipov, T.; Murphy, B.; Kukk, E.; Ueda, K.; Feifel, R.; Van der Meulen, P.; Salen, P.; Schmidt, H.; Thomas, R.D.; Larsson, M.; Richter, R.; Prince, K.C.; Bozek, J.D.; Bostedt, C.; Wada, S.-I.; Piancastelli, M.N.; Tashiro, M.; Ehara, M. *Proc. Nat. Acad. Sci. USA* **2011,** *108*, 16912–16915.

[24] Cryan, J.P.; Glownia, J.M.; Andreasson, J.; Belkacem, A.; Berrah, N.; Blaga, C.I.; Bostedt, C.; Bozek, J.; Buth, C.; DiMauro, L.F.; Fang, L.; Gessner, O.; Guehr, M.; Hajdu, J.; Hertlein, M.P.; Hoener, M.; Kornilov, O.; Marangos, J.P.; March, A.M.; McFarland, B.K.; Merdji, H. Petrovic´, V.S.; Raman, C.; Ray, D.; Reis, D.; Tarantelli, F.; Trigo, M.; White, J.L.; White, W.; Young, L.; Bucksbaum, P.H.; Coffee, R.N. *Phys. Rev. Lett.* **2010,** *105*, 083004.

[25] Fang, L.; Hoener, M.; Gessner, O.; Tarantelli, F.; Pratt, S.T.; Kornilov, O.; Buth, C.; Gühr, M.; Kanter, E.P.; Bostedt, C.; Bozek, J.D.; Bucksbaum, P.H.; Chen, M.; Coffee, R.; Cryan, J.; Glownia, M.; Kukk, E.; Leone, S.R.; Berrah, N. *Phys. Rev. Lett.* **2010,** *105*, 083005.

[26] Hoener, M.; Fang, L.; Kornilov, O.; Gessner, O.; Pratt, S.T.; Gühr, M.; Kanter, E.P.; Blaga, C.; Bostedt, C.; Bozek, J.D.; Bucksbaum, P.H.; Buth, C.; Chen, M.; Coffee, R.; Cryan, J.; DiMauro, L.; Glownia, M.; Hosler, E.; Kukk, E.; Leone, S.R.; McFarland, B.; Messerschmidt, M.; Murphy, B.; Petrovic, V.; Rolles, D.; Berrah, N. *Phys. Rev. Lett.* **2010,** *104*, 253002.

[27] Bostedt, C.; Eremina, E.; Rupp, D.; Adolph, M.; Thomas, H.; Hoener, M.; De Castro, A.R.B.; Tiggesbäumker, J.; Meiwes-Broer, K.-H.; Laarmann, T.; Wabnitz, H.; Plonjes, E.; Treusch, R.; Schneider, J.R. Moller. T. *Phys. Rev. Lett.* **2012,** *108*, 093401.

[28] Bostedt, C.; Adolph, M.; Eremina, E.; Hoener, M.; Rupp, D.; S., Schorb; Thomas, H.; De Castro, A.R.B.; Möller, T. *J. Phys. B: At. Mol. Opt. Phys.* **2010,** *43,* 194011.

[29] Thomas, H.; Helal, A.; Hoffmann, K.; Kandadai, N.; Keto, J.; Andreasson, J.; Iwan, B.; Seibert, M.; Timneanu, N.; Hajdu, J.; Adolph, M.; Gorkhover, T.; Rupp, D.; Schorb, S.; Moller, T.; Doumy, G.; DiMauro, L.F.; Hoener, M.; Murphy, B.; Berrah, N.; Messerschmidt, M.; Bozek, J.; Bostedt, C.; Ditmire, T. *Phys. Rev. Lett.* **2012,** *108*, 133401.

[30] Petrović, V.S.; Siano, M.; White, J.L.; Berrah, N.; Bostedt, C.; Bozek, J.D.; Broege, D.; Chalfin, M.; Coffee, R.N.; Cryan, J.; Fang, L.; Farrell, J.P.; Frasinski, L.J.; Glownia, J.M.; Guhr, M.; Hoener, M.; Holland, D.M.P.; Kim, J.; Marangos, J.P.; Martinez, T.; McFarland, B.K.; Minns, R.S.; Miyabe, S.; Schorb, S.; Sension, R.J.; Spector, L.S.; Squibb, R.; Tao, H.; Underwood, J.G.; Bucksbaum, P.H. *Phys. Rev. Lett.* **2012,** *108*, 253006.

[31] McFarland, B.K.; Farrell, J.P.; Miyabe, S.; Tarantelli, F.; Aguilar, A.; Berrah, N.; Bostedt, C.; Bozek, J.; Bucksbaum, P.H.; Castagna, J.C.; Coffee, R.N.; Cryan, J.P.; Fang, L.; Feifel, R.; Gaffney, K.J.; Glownia, J.M.; Martinez, T.J.; Mucke, M.; Murphy, B.; Natan, A.; Osipov, T.; Petrović, V.S.; Schorb, S.; Schultz, Th; Spector, L.S.; Swiggers, M.; Tenney, I.; Wang, S.; White, J.L.; White, W.; Gühr, M. *Nat. Commun.* **2014,** *5*, 4235.

[32] Neutze, R.; Wouts, R.; Van der Spoel, D.; Weckert, E.; Hajdu, J. *Nature* **2000,** *406,* 752–757.

[33] Barty, A.; Caleman, C.; Aquila, A.; Timneanu, N.; Lomb, L.; White, T.A.; Andreasson, J.; Arnlund, D.; Bajt, S.; Barends, T.R.M.; Barthelmess, M.; Bogan, M.J.; Bostedt, C.; Bozek, J.D.; Coffee, R.; Coppola, N.; Davidsson, J.; DePonte, D.P.; Doak, R.B.; Ekeberg, T.; Elser, V.; Epp, S.W.; Erk, B.; Fleckenstein, H.; Foucar, L.; Fromme, P.; Graafsma, H.; Gumprecht, L.; Hajdu, J.; Hampton, C.Y.; Hartmann, R.; Hartmann, A.; Hauser, G.; Hirsemann, H.; Holl, P.; Hunter, M.S.; Johansson, L.; Kassemeyer, S.; Kimmel, N.; Kirian, R.A.; Liang, M.; Maia, F.R.N.C.; Malmerberg, E.; Marchesini, S.; Martin, A.V.; Nass, K.; Neutze, R.; Reich, C.; Rolles, D.; Rudek, B.; Rudenko, A.; Scott, H.; Schlichting, I.; Schulz, J.; Seibert, M.M.; Shoeman, R.L.; Sierra, R.G.; Soltau, H.; Spence, J.C.H.; Stellato, F.; Stern, S.; Strüder, L.; Ullrich, J.; Wang, X.; Weidenspointner, G.; Weierstall, U.; Wunderer, C.B.; Chapman, H.N. *Nat. Photonics* **2012,** *6*, 35–40.

[34] Jurek, Z.; Faigel, G. *Europhys. Lett.* **2009,** *86,* 68003.

[35] Caleman, C.; Huldt, G.; Maia, F.R.N.C.; Ortiz, C.; Parak, F.G.; Hajdu, J.; Van der Spoel, D.; Chapman, H.N.; Timneanu, N. *ACS Nano* **2011,** *5,* 139–146.

[36] Barty, A.; Boutet, S.; Bogan, M.J.; Hau-Riege, S.; March-esini, S.; Sokolowski-Tinten, K.; Stojanovic, N.; Tobey, R.; Ehrke, H.; Cavalleri, A.; Düsterer, S.; Frank, M.; Bajt, S.C.; Woods, B.W.; Seibert, M.M.; Hajdu, J.; Treusch, R.; Chapman, H.N. *Nat. Photonics* **2008,** *2*, 415–419.

[37] Popmintchev, T.; Chen, M.-C.; Popmintchev, D.; Arpin, P.; Brown, S.; Ališauskas, S.; Andriukaitis, G.; Balčiunas, T.; Mücke, O.D.; Pugzlys, A.; Baltuška, A.; Shim, B.; Schrauth, S.E.; Gaeta, A.; Hernández-García, C.; Plaja, L.; Becker, A.; Jaron-Becker, A.; Murnane, M.M.; Kapteyn, H.C. *Science* **2012,** *336*, 1287–1291.

[38] Ullrich, J.; Rudenko, A.; Moshammer, R. *Annu. Rev. Phys. Chem.* **2012,** *63,* 635–660.

[39] Redecke, L.; Nass, K.; DePonte, D.P.; White, T.A.; Rehders, D.; Barty, A.; Stellato, F.; Liang, M.; Barends, T.R.M.; Boutet, S.; Williams, G.J.; Messerschmidt, M.; Seibert, M.M.; Aquila, A.; Arnlund, D.; Bajt, S.; Barth, T.; Bogan, M.J.; Caleman, C.; Chao, T.C.; Doak, R.B.; Fleckenstein, H.; Frank, M.; Fromme, R.; Galli, L.; Grotjohann, I.; Hunter, M.S.; Johansson, L.C.; Kassemeyer, S.; Katona, G.; Kirian, R.A.; Koopmann, R.; Kupitz, C.; Lomb, L.; Martin, A.V.; Mogk, S.; Neutze, R.; Shoeman, R.L.; Steinbrener, J.; Timneanu, N.; Wang, D.; Weierstall, U.; Zatsepin, N.A.; Spence, J.C.; Fromme, P.; Schlichting, I.; Duszenko, M.; Betzel, C.; Chapman, H.N. *Science* **2013,** *339*, 227–230.

[40] Boutet, S.; Lomb, L.; Williams, G.J.; Barends, T.R.M.; Aquila, A.; Doak, R.B.; Weierstall, U.; DePonte, D.P.; Steinbrener, J.; Shoeman, R.L.; Messerschmidt, M.; Barty, A.; White, T.A.; Kassemeyer, S.; Kirian, R.A.; Seibert, M.M.; Montanez, P.A.; Kenney, C.; Herbst, R.; Hart, P.; Pines, J.; Haller, G.; Gruner, S.M.; Philipp, H.T.; Tate, M.W.; Hromalik, M.; Koerner, L.J.; Bakel, N.V.; Morse, J.; Ghonsalves, W.; Arnlund, D.; Bogan, M.J.; Caleman, C.; Fromme, R.; Hampton, C.Y.; Hunter, M.S.; Johansson, L.S.; Katona, G.; Kupitz, C.; Liang, M.; Martin, A.V.; Nass, K.; Redecke, L.; Stellato, F.; Timneanu, N.; Wang, D.; Zatsepin, N.A.; Schafer, D.; Defever, J.; Neutze, R.; Fromme, P.; Spence, J.C.H.; Chapman, H.N.; Schlichting, I. *Science* **2012,** *337*, 362–364.

[41] Chapman, H.N.; Fromme, P.; Barty, A.; White, T.A.; Kirian, R.A.; Aquila, A.; Hunter, M.S.; Schulz, J.; DePonte, D.P.; Weierstall, U.; Doak, R.B.; Maia, F.R.N.C.; Martin, A.V.; Schlichting, I.; Lomb, L.; Coppola, N.; Shoeman, R.L.; Epp, S.W.; Hartmann, R.; Rolles, D.; Rudenko, A.; Foucar, L.; Kimmel, N.; Weidenspointner, G.; Holl, P.; Liang, M.; Barthelmess, M.; Caleman, C.; Boutet, S.; Bogan, M.J.; Krzywinski, J.; Bostedt, C.; Bajt, S.;

Gumprecht, L.; Rudek, B.; Erk, B.; Schmidt, C.; Hömke, A.; Reich, C.; Pietschner, D.; Strüder, L.; Hauser, G.; Gorke, H.; Ullrich, J.; Herrmann, S.; Schaller, G.; Schopper, F.; Soltau, H.; Kühnel, K.-U.; Messerschmidt, M.; Bozek, J.D.; Hau-Riege, S.P.; Frank, M.; Hampton, C.Y.; Sierra, R.G.; Starodub, D.; Williams, G.J.; Hajdu, J.; Timneanu, N.; Seibert, M.M.; Andreasson, J.; Rocker, A.; Jönsson, O.; Svenda, M.; Stern, S.; Nass, K.; Andritschke, R.; Schröter, C.-D.; Krasniqi, F.; Bott, M.; Schmidt, K.E.; Wang, X.; Grotjohann, I.; Holton, J.M.; Barends, T.R.M.; Neutze, R.; Marchesini, S.; Fromme, R.; Schorb, S.; Rupp, D.; Adolph, M.; Gorkhover, T.; Andersson, I.; Hirsemann, H.; Potdevin, G.; Graafsma, H.; Nilsson, B.; Spence, J.C.H. *Nature* **2011,** *470*, 73–77.

[42] Seibert, M.M.; Ekeberg, T.; Maia, F.R.N.C.; Svenda, M.; Andreasson, J.; Jönsson, O.; Odić, D.; Iwan, B.; Rocker, 95 A.; Westphal, D.; Hantke, M.; DePonte, D.P.; Barty, A.; Schulz, J.; Gumprecht, L.; Coppola, N.; Aquila, A.; Liang, M.; White, T.A.; Martin, A.; Caleman, C.; Stern, S.; Abergel, C.; Seltzer, V.; Claverie, J-M.; Bostedt, C.; Bozek, J.D.; Boutet, S.; Miahnahri, A.A.; Messerschmidt, M.; Krzywinski, J.; Williams, G.; Hodgson, K.O.; Bogan, M.J.; Hampton, C.Y.; Sierra, R.G.; Starodub, D.; Andersson, I.; Bajt, S.; Barthelmess, M.; Spence, J.C.H.; Fromme, P.; Weierstall, U.; Kirian, R.; Hunter, M.; Doak, R.B.; Marchesini, S.; Hau-Riege, S.P.; Frank, M.; Shoeman, R.L.; Lomb, L.; Epp, S.W.; Hartmann, R.; Rolles, D.; Rudenko, A.; Schmidt, C.; Foucar, L.; Kimmel, N.; Holl, P.; Rudek, B.; Erk, B.; Hömke, A.; Reich, C.; Pietschner, D.; Weidenspointner, G.; Strüder, L.; Hauser, G.; Gorke, H.; Ullrich, J.; Schlichting, I.; Herrmann, S.; Schaller, G.; Schopper, F.; Soltau, H.; Kühnel, K-U.; Andritschke, R.; Schröter, C-D.; Krasniqi, F.; Bott, M.; Schorb, S.; Rupp, D.; Adolph, M.; Gorkhover, T.; Hirsemann, H.; Potdevin, G.; Graafsma, H.; Nilsson, B.; Chapman, H.N.; Hajdu, J. *Nature* **2011,** *470,* 78–81.

[43] Owen, R.L.; Rudiño-Piñera, E.; Garman, E.F. *Proc. Nat. Acad. Sci. USA* **2006,** *103,* 4912–4917.

[44] Lomb, L.; Barends, T.R.M.; Kassemeyer, S.; Aquila, A.; Epp, S.W.; Erk, B.; Foucar, L.; Hartmann, R.; Rudek, B.; 100 Rolles, D.; Rudenko, A.; Shoeman, R.L.; Andreasson, J.; Bajt, S.; Barthelmess, M.; Barty, A.; Bogan, M.J.; Bostedt, C.; Bozek, J.D.; Caleman, C.; Coffee, R.; Coppola, N.; DePonte3, D.P.; Doak, R.B.; Ekeberg, T.; Fleckenstein, H.; Fromme, P.; Gebhardt, M.; Graafsma, H.; Gumprecht, L.; Hampton, C.Y.; Hartmann, A.; Hauser G.; Hirsemann, H.; Holl, P.; Holton, J.M.; Hunter, M.S.; Kabsch, W.; Kimmel, N.; Kirian, R.A.; Liang, M.; Maia, F.R.N.C.; Meinhart, A.; Marchesini, S.; Martin, A.V.; Nass, K.; Reich, C.; Schulz, J.; Seibert, M.M.; Sierra, R.; Soltau, H.; Spence, J.C.H.; Steinbrener, J.; Stellato, F.; Stern, S.; Timneanu, N.; Wang, X.; Weidenspointner, G.; Weierstall, U.; White, T.A.; Wunderer, C.; Chapman, H.N.; Ullrich, J.; Strüder, L.; Schlichting, I. *Phys. Rev. B.* **2011,** *84,* 214111.

[45] Johansson, O.; Bohl, E.; Henderson, G.G.; Mignolet, B.; Dennis, T.J.S.; Remacle, F.; Campbell, E.E.B. *J. Chem. Phys.* **2013,** *139,* 084309.

[46] Bozek, J.D. *Eur. Phys. J. Special Topics* **2009,** *169,* 129–132.

[47] Pešić, Z.D.; Rolles, D.; Perri, M.; Bilodeau, R.C.; Ackerman, G.D.; Rude, B.S.; Kilcoyne, A.L.D.; Bozek, J.D.; Berrah, N. *J. Elec. Spect. Rel. Phen.* **2007,** *155,* 155–159.

[48] Bartels, R.; Backus, S.; Zeek, E.; Misoguti, L.; Vdovin, G.; Christov, I.P.; Murnane, M.M.; Kapteyn, H.C. *Nature* **2000,** *406,* 164–166.

[49] *At. Data Nucl. Data Tables*. **1993,** *54,* 181–342. http://ulisse.elettra.trieste.it/services/elements/WebElements

[50] Kornilov, O.; Eckstein, M.; Rosenblatt, M.; Schulz, C.P.; Motomura, K.; Rouzée, A.; Klei, J.; Foucar, L.; Siano, M.; Lübcke, A.; Schapper, F.; Johnsson, P.; Holland, D.M.P.; Schlathölter, T.; Marchenko, T.; Düsterer, S.; Ueda, K.; Vrakking, M.J.J.; Frasinski, L.J. *J. Phys. B: At. Mol. Opt. Phys.* **2013,** *46,* 164028.

[51] Zhaunerchyk, V.; Mucke, M.; Salén, P.; Meulen, P.V.D.; Kaminska, M.; Squibb, R.J.; Frasinski, L.J.; Siano, M.; Eland, J.H.D.; Linusson, P.; Thomas, R.D.; Larsson, M.; Foucar, L.; Ullrich, J.; Motomura, K.; Mondal, S.; Ueda, K.; Osipov, T.; Fang, L.; Murphy, B.F.; Berrah, N.; Bostedt, C.; Bozek, J.D.; Schorb, S.; Messerschmidt, M.; Glownia, J.M.; Cryan, J.P.; Coffee, R.N.; Takahashi, O.; Wada, S.; Piancastelli, M.N.; Richter, R.; Prince, K.C.; Feifel, R. *J. Phys. B: At. Mol. Opt. Phys.* **2013,** *46*, 164034.

[52] Sahnoun, R.; Nakai, K.; Sato, Y.; Kono, H.; Fujimura, Y.; Tanaka, M. *Chem. Phys. Lett.* **2006,** *430,* 167–172.

[53] Wolf, M.; Müller, K.-H.; Skourski, Y.; Eckert, D.; Georgi, P.; Krause, M.; Dunsch, L. *Angew. Chem. Int. Ed.* **2005,** *44,* 3306–3309.

[54] Yang, S.; Troyanov, S.I.; Popov, A.A.; Krause, M.; Dunsch, L. *J. Am. Chem. Soc*. **2006,** *128,* 16733–16739.

[55] Zhang, Y.; Krylov, D.; Schiemenz, S.; Rosenkranz, M.; Westerström, R.; Dreiser, J.; Greber, T.; Büchner, B.; Popov, A.A. *Nanoscale* **2014,** *6,* 11431–11438.

[56] Zewail, A.H. *Angew. Chem. Int. Ed.* **2000,** *39,* 2586–2631.

[57] Sansone, G.; Kelkensberg, F.; Morales, F.; Perez-Torres, J.F.; Martín, F.; Vrakking, M.J.J. *IEEE J. Sel. Top. Quantum Electron.* **2012,** *18,* 520–530.

[58] Liekhus-Schmaltz, C.E.; Tenney, I.; Osipov, T.; Sanchez-Gonzalez, A.; Berrah, N.; Boll, R.; Bomme, C.; Bostedt, C.; Bozek, J.D.; Carron, S.; Coffee, R.; Devin, J.; Erk, B.; Ferguson, K.R.; Field, R.W.; Foucar, L.; Frasinski, L.J.; Glownia, J.M.; Gühr, M.; Kamalov, A.; Krzywinski, J.; Li, H.; Marangos, J.P.; Martinez, T.J.; McFarland, B.K.; Miyabe, S.; Murphy, B.; Natan, A.; Rolles, D.; Rudenko, A.; Siano, M.; Simpson, E.R.; Spector, L.; Swiggers, M.; Walke, D.; Wang, S.; Weber, T.; Bucksbaum, P.H.; Petrovic, V. *Nat. Commun.,* accepted for publication, **2015**.

[59] Glownia, J.M.; Cryan, J.; Andreasson, J.; Belkacem, A.; Berrah, N.; Blaga, C.I.; Bostedt, C.; Bozek, J.; DiMauro, L.F.; Fang, L.; Frisch, J.; Gessner, O.; Gühr, M.; Hajdu, J.; Hertlein, M.P.; Hoener, M.; Huang, O.; Kornilov, J.P.; Marangos, A.M.; March, B.K.; McFarland, H.; Merdji, V.S.; Petrovic, C.; Raman, G.; Ray, D.; Reis, D.A.; Trigo, M.; White, J.L.; White, W.; Wilcox, R.; Young, L.; Coffee, R.N.; Bucksbaum, P.H. *Opt. Express* **2010,** *18*, 17620–17630.

[60] Schnorr, K.; Senftleben, A.; Kurka, M.; Rudenko, A.; Foucar, L.; Schmid, G.; Broska, A.; Pfeifer, T.; Meyer, K.; Anielski, D.; Boll1, R.; Rolles, D.; Kübel, M.; Kling, M.F.; Jiang, Y.H.; Mondal, S.; Tachibana, T.; Ueda, K.; Marchenko, T.; Simon, M.; Brenner, G.; Treusch, R.; Scheit, S.; Averbukh, V.; Ullrich, J.; Schröter, C.D.; Moshammer, R. *Phys. Rev. Lett.* **2013,** *111,* 093402.

[61] Castagna, J.C.; Murphy, B.; Bozek, J.; Berrah, N. *J. Phys: Conf. Ser.* **2013,** *425,* 152021.

[62] Yumoto, H.; Mimura, H.; Koyama, T.; Matsuyama, S.; Tono, K.; Togashi, T.; Inubushi, Y.; Sato, T.; Tanaka, T.; Kimura, T.; Yokoyama, H.; Kim, J.; Sano, Y.; Hachisu, Y.; Yabashi, M.; Ohashi, H.; Ohmori, H.; Ishikawa, T.; Yamauchi, K. *Nat. Photonics* **2013,** *7,* 43–47.

[63] Osipov, T.; Rolles, D.; Bostedt, C.; Castagna, J.-C.; Hartmann, R.; Bozek, J.D.; Schlichting, I.; Strüder, L.; Ullrich, J.; Berrah, N. *Bull. Am. Phys. Soc.* **2011,** *134,* 87.
[64] Ding, Y.; Brachmann, A.; Decker, F.-J.; Dowell, D.; Emma, P.; Frisch, J.; Gilevich, S.; Hays, G.; Hering, Ph.; Huang, Z.; Iverson, R.; Loos, H.; Miahnahri, A.; Nuhn, H.-D.; Ratner, D.; Turner, J.; Welch, J.; White, W.; Wu, J. *Phys. Rev. Lett.* **2009,** *102*, 254801.
[65] Amann, J.; Berg, W.; Blank, V.; Decker, F.-J.; Ding, Y.; Emma, P.; Feng, Y.; Frisch, J.; Fritz, D.; Hastings, J.; Huang, Z.; Krzywinski, J.; Lindberg, R.; Loos, H.; Lutman, A.; Nuhn, H.-D.; Ratner, D.; Rzepiela, J.; Shu, D.; Shvyd'ko, Yu; Spampinati, S.; Stoupin, S.; Terentyev, S.; Trakhtenberg, E.; Walz, D.; Welch, J.; Wu, J.; Zholents, A.; Zhu, D. *Nat. Photonics* **2012,** *6*, 693–698.
[66] Wöstmann, M.; Mitzner, R.; Noll, T.; Roling, S.; Siemer, B.; Siewert, F.; Eppenhoff, S.; Wahlert, F.; Zacharias, H. *J. Phys. B: At. Mol. Opt. Phys.* **2013,** *46,* 164005.
[67] Berrah, N.; Fang, L.; Murphy, B.; Castagna, J.C.; Kukk, E.; Xiong, H.; Bozek, J.D. *J. Elect. Spectros. Relat. Phenom.* **2014,** *196*, 34–37.